Reproductive Toxicology 98 (2020) 107–116

Contents lists available at ScienceDirect

Reproductive Toxicology

journal homepage: www.elsevier.com/locate/reprotox

An efficient neuron-astrocyte differentiation protocol from human embryonic stem cell-derived neural progenitors to assess chemical-induced developmental neurotoxicity

Victoria C. de Leeuw [a,b,1,*], Conny T.M. van Oostrom [a,1], Remco H.S. Westerink [b], Aldert H. Piersma [a,b], Harm J. Heusinkveld [a], Ellen V.S. Hessel [a]

[a] Centre for Health Protection, National Institute for Public Health and the Environment (RIVM), Bilthoven, the Netherlands
[b] Institute for Risk Assessment Sciences (IRAS), Utrecht University, Utrecht, the Netherlands

ARTICLE INFO

Keywords:
Developmental neurotoxicity
Human stem cells
Embryonic stem cells
Nervous system
In vitro
3Rs

ABSTRACT

Human embryonic stem cell neuronal differentiation models provide promising *in vitro* tools for the prediction of developmental neurotoxicity of chemicals. Such models mimic essential elements of human relevant neuronal development, including the differentiation of a variety of brain cell types and their neuronal network formation as evidenced by specific gene and protein biomarkers. However, the reproducibility and lengthy culture duration of cell models present drawbacks and delay regulatory implementation. Here we present a relatively short and robust protocol to differentiate H9-derived neural progenitor cells (NPCs) into a neuron-astrocyte co-culture. When frozen-stored NPCs were re-cultured and induced into neuron-astrocyte differentiation, they showed gene- and protein expression typical for these cells, and most notably they exhibited spontaneous electrical activity within three days of culture as measured by a multi-well micro-electrode array. Modulating the ratio of astrocytes and neurons through different growth factors including glial cell line-derived neurotrophic factor (GDNF), brain-derived neurotrophic factor (BDNF), and ciliary neurotrophic factor (CNTF) did not compromise the ability to develop spontaneous electrical activity. This robust neuronal differentiation model may serve as a functional component of a testing strategy for unravelling mechanisms of developmental neurotoxicity.

1. Introduction

Development of the central nervous system is extremely complex, involving many different processes at the molecular, cellular and tissue level. These processes include for example neurogenesis, migration, axon guidance, synaptogenesis, myelination, phenotypic specification of neurons, expression and maturation of receptors and ion channels, and brain segmentation [1–3]. Disruption of these processes can influence the development of motor deficiencies or behavioural conditions such as autism spectrum disorder, intellectual disability and attention-deficit hyperactivity disorder [4].

The developing nervous system has unique and specific windows of vulnerability. The exact mechanisms and aetiologies of neurodevelopmental disorders are commonly unknown, but exposure to environmental chemicals may be contributing [5]. Regulatory developmental neurotoxicity (DNT) testing is done using animal based test guidelines (OECD TG-426, 443 [6,7]) [6,7]. However, given the complexity of the human brain, the predictivity of these animal tests for human health is limited. This notion has stimulated research into human relevant *in vitro* and *in silico* test methods for DNT. From the perspective of coverage of all relevant processes in the human brain development, one-in-one replacement of *in vivo* tests by relatively simple *in vitro* assays is not feasible. A testing strategy for DNT prediction covering all the essential processes in human brain development is needed based on a combination of human-relevant, robust and reproducible *in vitro* and *in silico* test. A multitude of alternative models have been developed over the years, providing insights into mechanisms of action of chemicals [8]. Most of these models, however, measure structural readouts such as proliferation, differentiation, migration and neurite outgrowth, but do not assess neuronal function readouts, which could provide evidence for

* Corresponding author at: National Institute for Public Health and Environment (RIVM), Centre for Health Protection (GZB), Antonie van Leeuwenhoeklaan 9, 3721 MA Bilthoven, the Netherlands.
E-mail address: victoria.de.leeuw@rivm.nl (V.C. de Leeuw).
[1] Contributed equally.

https://doi.org/10.1016/j.reprotox.2020.09.003
Received 15 June 2020; Received in revised form 13 August 2020; Accepted 7 September 2020
Available online 12 September 2020

DNT at a higher level of integration. Neuronal function readouts include for example network formation, inter- and intracellular signalling and electrical activity, for which proper synaptogenesis is essential [9,10]. Synaptogenesis is a critical process whereby neurons establish specialised contact sites, which facilitate neuronal communication [9]. The accumulation of presynaptic proteins (e.g., synapsin, synaptophysin) in close proximity to post-synaptic density proteins (e.g., PSD95) in the dendrites of neighbouring neurons are essential morphological features associated with synaptogenesis [9,11,12].

Functional neuronal network development *in vitro* has proved challenging as spontaneous electrical activity was difficult to measure and/or differentiation took several weeks [13–18]. These drawbacks represent important limitations for implementation in regulatory testing.

Human embryonic stem cell differentiation protocols provide a continuous source of human neurons and astrocytes. These neuronal cultures can be used to analyse chemical disruption at different levels, from gene expression modulation to structural and morphological effects [19]. The addition of functional neuronal network characteristics, including synaptogenesis and electrical activity, in a robust cell culture model would provide added value for DNT assessment and mechanistic studies [20].

In this study a human stem cell based *in vitro* model is presented, which represents the differentiation of neural progenitors into a spontaneously firing neuron-astrocyte co-culture within three days of culture. The aim of this study was to examine the characteristics of this human stem cell neural network differentiation model and to define the biological domain of the model by measuring key elements of synaptogenesis and spontaneous electrical activity. This functional neuronal differentiation protocol may serve as an important component in a human relevant testing strategy for the animal-free assessment of DNT of chemicals and pharmaceuticals based on mechanistic knowledge of human biology and physiology of brain development.

2. Materials and methods

All reagents were bought at Gibco (Waltham, MA, USA) unless mentioned otherwise.

2.1. Neuronal differentiation of embryonic stem cells

2.1.1. hESC maintenance

H9 human embryonic stem cells (WA09, passage 26, WiCell, Madison, WI, USA) were thawed and seeded at a density of 1×10^6 on Vitronectin (VTN-N; 5 ng/mL) coated 6-well plates (Corning, Corning, NY, USA) in Essential 8 Flex medium according to Gibco's Essential 8 Flex protocol (Document MAN0013988 version 1.0, Gibco). Cells were kept in a humidified chamber (37 °C, 5% CO_2, 20 % O_2) and passaged at a split ratio of 1:2−1:4 every 3–4 days when cells reached 80–90 % confluency. Instead of two washes with DPBS, cells were rinsed once with Versene solution and subsequently incubated with Versene solution for 7 min at room temperature (RT) to dissociate the cells. Stem cells with passage numbers 49–60 were used for differentiation experiments to ensure that continuous culturing in E8 medium for multiple passages resulted in a pure stem cell culture without too much contamination with other cells.

2.1.2. Neural progenitors (NPCs) generation from hESCs

Induction of differentiation was performed according to a neuronal induction protocol from Stemcell (Document #28782, Stemcell Technologies, Vancouver, Canada), with the exception that from this moment all steps were performed in 3% O_2 to enhance neuronal differentiation [21,22]. The protocol comprised three steps: embryoid body (EB) generation, neural rosette formation and neural progenitor (NPC) expansion.

When confluent, stem cells were incubated with Gentle Cell Dissociation Reagent for 9 min, dissociated and replated at a density of 3×10^6 cells/mL in a AggreWell™800 24-well plate in STEMdiff™ Neural Induction (NI) medium + SMADi supplemented with 10 μM Y-27632 (all from Stemcell). Half of the medium was replaced every day until day 5. EBs were then transferred to Poly-L-Ornithine (PLO, 15 μg/mL, Sigma) / laminin (10 μg/mL, Sigma) coated a 6-well plate (Corning) in STEMdiff™ Neural Induction Medium + SMADi (Stemcell) to form neural rosettes. Medium was fully changed on a daily basis for seven days. On day 12 of differentiation, neural rosettes were selected by incubating the cells for 1.5 h in Neural Rosette Selection Reagent (Stemcell) and replated on PLO/laminin dishes for another seven days. A second rosette selection round was performed on day 19 following the same procedure as on day 12 and rosettes were transferred to fresh PLO/laminin 6-well plates (Corning) to grow until confluent (~one week), refreshing the whole medium every day. Around day 26, cells were rinsed once with DMEM/F12 medium and dissociated by incubating with StemPro™ Accutase™ Cell Dissociation Reagent for 7 min and transferred at a density of $1.2–1.5 \times 10^6$ cells/mL in STEMdiff™ Neural progenitor (NP) medium (Stemcell) on PLO/laminin coated 6-well plates (p1 NPCs). NPCs received daily complete medium changes and were passaged when they reached confluency (~one week) according to the NPC passaging protocol. NPCs were frozen at a density of $2–8 \times 10^6$ cells/mL according to the Freezing protocol in STEMdiff™ Neural progenitor Freezing Medium (Stemcell) and stored in liquid nitrogen until use for neuron-astrocyte generation.

2.1.3. Neuron-astrocyte generation cell culture

Two media were used for neuron-astrocyte generation to determine the optimal medium composition. The medium from Pistollato et al. ([23]; hereafter called P-) comprised neurobasal medium supplemented with 10 μl/mL N2 supplement, 20 μl/mL B-27 supplement, 10 μl/mL 5000 IU/mL Penicillin / 5000 μg/mL Streptomycin, 1 ng/mL glial cell line-derived neurotrophic factor (GDNF) and 2.5 ng/mL brain-derived neurotrophic factor (BDNF). The medium adopted from Gunhanlar et al. ([24]; hereafter called G-) consisted of neurobasal medium, 10 μl/mL N2 supplement, 20 μl/mL B-27-retinoic acid supplement, 10 μl/mL5000 IU/mL Penicillin / 5000 μg/mL Streptomycin, 10 μl/mL nonessential amino acids, 20 ng/mL GDNF, 20 ng/mL BDNF, 1 μM dibutyryl cyclic adenosine monophosphate (Sigma-Aldrich), 200 μM ascorbic acid (Sigma-Aldrich) and 2 μg/mL laminin (Sigma-Aldrich). Ciliary neurotrophic factor (CNTF) was added to both media to a final concentration of 10 ng/mL to create a version of the media that promotes astroglial growth (P + and G+).

When NPCs were thawed from the freezer, cells were grown for six days before replating for neuron-astrocyte generation. NPCs were seeded 2.56×10^5 cells/cm^2 on PLO/laminin-coated 48-well multi-well micro-electrode arrays (mwMEA, Axion Biosystems Inc., Atlanta, GA, USA) for MEA measurements, 8-well micro-slides (Ibidi, Gräfelfing, Germany) for immunocytochemistry or 12-well plates (Corning) for qPCR, depending on application. NPCs were cultured in the presence of NP medium for one day after which the medium was replaced by differentiation medium. Except for MEA-applications, cells were kept in low oxygen conditions (3% O_2). Medium replacements took place every 2–3 days and cultures were continued for up to four weeks.

2.2. Immunocytochemistry

Samples were rinsed with PBS and fixed for 30 min with 4% prewarmed paraformaldehyde (Electron Microscopy Sciences, Hatfield, PA, USA) in PBS. Cells were permeabilised for 5 min with 0.2 % (Table 1, protocol A) or 0.5 % (protocol B) Triton X-100 (Sigma-Aldrich) in PBS. Blocking was performed either in 1% bovine serum albumin (BSA; w/v; Sigma-Aldrich), 0.5 % Tween-20 (Sigma-Aldrich) in PBS for 1 h at 37 °C (protocol A) or in 5% BSA (Sigma-Aldrich) for 30 min at RT(protocol B), depending on the antibody used (Table 1). Primary antibodies were applied overnight at 4 °C in 0.5 % BSA/0.5 % Tween-20 in PBS (protocol A) or 5% normal goat serum (v/v, Sigma-Aldrich)/0.5 % Tween-20

Table 1
Primary and secondary antibodies.

Antibody	Abbreviation	Marker for	Product number	Company	Dilution	Protocol
Mouse anti Stage Specific Embryonic Antigen-4	SSEA4	Stem cell	MAB4304	Millipore	1:250	A
Rat anti E-cadherin	ECAD	Adhesion molecule present before neuronal tube closure	13−1900	Invitrogen	1:1000	A/B
Rabbit anti Paired homeobox 6	PAX6	Neural progenitor	901,301	Biolegend	1:1000	A/B
Mouse anti Zonula occludens-1	ZO-1	Tight junction protein typical in neuronal induction	33−9100	Thermo Fischer	1:1000	A
Rabbit anti β-Tubulin III	TUBB3	Neuron	T2200	Sigma-Aldrich	1:1000	A/B
Mouse anti Microtubule-associated protein 2	MAP2	Neuron, dendrite-specific	801,801	Biolegend	1:2000	A/B
Guinea pig anti Tau	TAU	Neuron, axon specific	314 004	Synaptic Systems	1:1000	A/B
Rat anti Glial fibrillary acidic protein	GFAP	Early astrocyte	13−0300	Invitrogen	1:800	A/B
Guinea pig anti- Vesicular glutamate transporter 2	VGLUT2	Synaptic vesicle excitatory neuron	AB2251-I	Millipore	1:2000	A
Mouse anti vesicular GABA transporter	VGAT	Synaptic vesicle inhibitory neuron	131,011	Synaptic Systems	1:500	B
Mouse anti postsynaptic density 95	PSD95	Post-synapse	MAB1598	Merck	1:500	B
Rabbit anti synaptoporin	SYNPR	Pre-synapse	102,002	Synaptic Systems	1:500	A
Goat anti rabbit Alexa 488			A11034	Invitrogen	1:1000	
Goat anti guinea pig Alexa 488			A11073	Invitrogen	1:1000	
Goat anti rabbit Alexa 555			A21429	Invitrogen	1:500	
Goat anti mouse Alexa 555			A21424	Invitrogen	1:1000	
Goat anti rat Alexa 555			A21434	Invitrogen	1:200	
Goat anti mouse Alexa 647			A21236	Invitrogen	1:500	

(Sigma-Aldrich) in PBS (protocol B). After washing away the primary antibodies, secondary antibodies were applied for 1 h in the same antibody incubation mixture. DAPI (Sigma-Aldrich) was used to stain nuclei of the cells. Imaging was performed on a Leica DMi8 microscope system (Leica, Wetzlar, Germany) using the appropriate Leica Software (LAS X). Images were further processed in ImageJ (version 1.51n; Rasband, 1997–2018 [25]).

2.3. RNA isolation and qPCR

Medium from samples (hESC n = 4, EB/NPC n = 2, Rosette n = 3, P-/P + n = 5, G- n = 6, G + n = 7; all technical replicates from one continuous experiment) was aspirated, cells were fixed in QIAzol (Qiagen, Hilden, Germany) and stored at −80 °C until further processing. Samples were ran through a QIAshredder (Qiagen) prior to RNA isolation to homogenise samples and whole RNA extraction was performed according to the manufacturer's protocol with the RNeasy® mini kit, including the DNase digestion step (Qiagen, version October 2019). Concentration of RNA was determined using the NanoDrop™ 1000 spectrophotometer (Nanodrop Technologies, Wilmington, DE, USA) and the 2100 Bioanalyzer (Agilent Technologies, Amstelveen, the Netherlands) to determine the quality of the samples. Synthesis of cDNA was performed using the cDNA archive kit consisting of random hexamer primers (Applied Biosystems, Foster City, CA, USA). Subsequent qPCR was done using a 7500 Fast Real-Time PCR system (Applied Biosystems; thermal cycling conditions: 95 °C for 20 s, 40 cycles of 95 °C for 3 s, 60 °C for 30 s). The primers used are summarised in Table 2. Relative gene expression differences were calculated using the $2^{-\Delta\Delta Ct}$ -method [26], normalised against the housekeeping genes Hypoxanthine phosphoribosyltransferase 1 (*HPRT1*) and Glucuronidase beta (*GUSB*). Statistical analysis was performed in GraphPad Prism (version 8.2.1) using a one-way ANOVA test and post-hoc Sidak's multiple comparisons test.

2.4. MEA measurements during neuron-astrocyte generation

To assess whether the combined expression of synaptic markers in the different neuron-astrocyte cultures resulted in functional connections, cultures were screened for the development of spontaneous electrical activity starting three days after the initiation of neuronal differentiation. Cultures were grown mwMEA plates as mentioned in Section 2.1.3 with each well containing 16 individual embedded nanotextured gold microelectrodes, yielding a total of 768 channels (Axion Biosystems Inc., Atlanta, GA, USA). Recordings were made as previously described [27] every two to three days for 30 days. Briefly, a 48-wells mwMEA plate was placed into the Maestro 768-channel amplifier with integrated heating system, temperature controller (set at 37 °C) and data acquisition interface (Axion BioSystems Inc.). After a 5 min stabilisation period, a 30 min recording of spontaneous activity was started. All

Table 2
Primers used for gene expression with corresponding marker function and assay ID. All primers were bought from Applied Biosystems.

Gene name	Abbreviation	Marker for	Assay ID
POU Class 5 Homeobox 1	*POU5F1*	Stem cell	Hs00999632_g1
Neurogenin 1	*NEUROG1*	Neural ectoderm	Hs01029249_s1
Nestin	*NES*	Neural progenitor	Hs00707120_s1
Tubulin, beta 3 class III	*TUBB3*	Neuron	Hs00801390_s1
Microtubule-associated protein 2	*MAP2*	Mature neuron	Hs00258900_m1
Synaptoporin	*SYNPR*	Pre-synapse	Hs01548398_m1
Discs Large MAGUK Scaffold Protein 4	*DLG4*	Post-synapse	Hs01555373_m1
Vesicular glutamate transporter	*SLC17A6*	Excitatory neuron	Hs00220439_m1
Vesicular inhibitory amino acid transporter	*SLC32A1*	Inhibitory neuron	Hs00369773_m1
Glial fibrillary acidic protein	*GFAP*	Early astrocyte	Hs00909233_m1
Glucuronidase beta	*GUSB*	Housekeeping gene	Hs00939627_m1
Hypoxanthine phosphoribosyltransferase 1	*HPRT1*	Housekeeping gene	Hs02800695_m1

culture conditions were tested in at least two independent cultures from one NPC bank and reproduced in a NPC bank generated from another H9 aliquot. Data acquisition was performed using Axion's Integrated Studio (AxIS, version 1.7.8) and channels were sampled at 12.5 kHz. Signals were pre-amplified with a gain of 1200 × (61 dB) and band-pass filtered at 0.2–5 kHz. This raw data was re-recorded and spikes were detected using the AxIS spike detector (Adaptive threshold crossing, Ada BandFit version 2) with a post/pre spike duration of 3.6/2.4 ms and a spike threshold of 6 × SD of the internal noise level (rms) of each individual electrode. Subsequent sorting and analysis of the re-recorded data was performed using custom-made Excel macros.

Data on spontaneous electrical activity was presented as mean spike rate (MSR; average number of spikes per second per well) and weighted mean burst rate (MBR; average number of bursts per second per active well) obtained from two (Pistollato protocols) or three (Gunhanlar protocols) independent experiments with 10–12 wells per culture condition.

3. Results

3.1. Differentiating H9 cells into neural progenitors and a neuron-astrocyte co-culture

The neuronal differentiation protocol consisted of two components: A) NPC generation consisting of four stages (1: H9, 2: EB, 3: Rosettes, 4: NPCs) and B) Neuron-astrocyte generation (stage 5: Neurons-astrocytes), which are depicted in a time line with representative images in Fig. 1A and B.

3.1.1. NPC generation and characterisation

EBs were formed from H9 stem cells from day 0 to day 5. The H9 stem cell culture consisted predominantly of stem cells as shown by stem cell marker SSEA-4 and pre-neural tube tight junction marker ECAD with a few cells that entered the differentiation process indicated by PAX6$^+$ cells, a marker for neural progenitors (Fig. 1C; H9). This was confirmed by gene expression of stem cell marker *POU5F1*, which was relatively highly expressed in stem cell culture in comparison to the differentiation stages. Gene expression of early and late neuronal differentiation markers (*NEUROG1, NESTIN*, *TUBB3, MAP2*, *GFAP*) was low in the stem cell culture compared to the other stages of differentiation (Fig. 1D). After EB formation, individual EBs grew out into neural rosettes over the course of one week (day 5–12). In order to obtain a more homogeneous NPC culture, neural rosettes were selected and replated to grow as rosettes for a second time (day 12–19). This step was repeated on day 19 and cells were grown as NPCs for one week (day 19–26) before further expansion to freeze down the cells or start neuron-astrocyte generation cultures. Neural rosettes were positively stained for PAX6 (Fig. 1C; Rosettes) and some cells also expressed neuronal marker TUBB3 (data not shown). Tight junction ZO-1 completely replaced ECAD and was specifically expressed on the apical side of the rosettes, analogous to expression of ZO-1 on the inside of the neural tube. Gene expression patterns corroborated the immunostainings, showing a large increase of early neurogenesis marker *NEUROG1*, neural progenitor marker *NESTIN* and neuronal markers *TUBB3* and *MAP2* (Fig. 1D). NPCs presented a mix of PAX6$^+$ and TUBB3$^+$ cells, whereby the PAX6 expression was markedly lower than in the rosette stage, indicating that the NPC culture already contained some differentiating neurons (Fig. 1C; NPCs). *NEUROG1* gene expression peaked at this point in time while *NESTIN* expression stabilised and *TUBB3* and *MAP2* expression steadily increased (Fig. 1D).

3.1.2. Neuron-astrocyte generation and characterisation

Two protocols were chosen to initiate neuron-astrocyte generation in order to assess the optimal protocol for the generation of a functional neuronal network, from Pistollato et al. [23] (P-) and Gunhanlar et al. [24] (G-), as described in Section 2.1.3. Two other conditions were created by adding CNTF to each of the media to stimulate the growth of astrocytes (P + and G+).

In all four neuron-astrocyte generation protocols a clear increase in neuronal markers was seen, which is apparent from representative images for all protocols at day 14 and 28 (Fig. 1C). After fourteen days, a mixed neuron-astrocyte culture had developed, expressing some PAX6$^+$ cell populations, maturing neurons shown by TAU$^+$ axons and MAP2$^+$ dendrites (Fig. 1C; Neurons day 14), and astrocytes (GFAP, data shown in Fig. 3). *GFAP* gene expression increased dramatically at this point, while *TUBB3* and *MAP2* expression steadily increased further and *NEUROG1* expression decreased, indicating that the cell culture was maturing at this point (Fig. 1D). Two weeks later, GFAP$^+$ astrocytes became more predominant and neurotransmitter transporters such as VGLUT2 were abundantly present (Fig. 1C; Neurons day 28).

3.2. Neuron-astrocyte cultures expressed transporters and synaptic markers indicative for synaptogenesis

The gene expression of pre-synaptic marker *SYNPR*, post-synaptic marker *DLG4*, and vesicular transporters for excitatory glutamate *SLC17A6* and inhibitory GABA *SLC32A1* were measured at each of the differentiation stages (Fig. 2A). Each of the markers presented a distinct expression pattern over time. *SYNPR* expression initially dropped upon differentiation and increased only in the neuron-astrocyte generation stage, while expression of *SLC32A1* was already upregulated from the NPC stage. *SLC17A6* gene expression was increased even earlier in the rosettes and *DLG4* expression steadily increased from the earliest time points on. Immunocytochemistry of the neuron-astrocyte culture on day 14 confirmed the presence of all of the synaptic and transporter markers. VGAT (encoded by *SCL32A1*) was only present in some neurites (Fig. 2B), while SYNPR, PSD95 (encoded by *DLG4*) and VGLUT2 (encoded by *SLC17A6*) were abundantly present throughout the cell culture (Fig. 2C, D).

There were no obvious differences in protein expression between the four neuron-astrocyte generation protocols P-/P+/G-/G+ (data not shown). Also with regard to overall trends in gene expression of synaptic- and transporter markers there were no major differences between the four protocols. No statistically significant differences were found between P- and G-, and between P + and G + protocols, indicating that all protocols resulted in a comparable distribution of these markers. The addition of CNTF to each of the protocols, however, resulted in lower gene expression of *SYNPR*, *DLG4* and *SLC17A6*, and a trend in lower *SLC32A1* expression compared to the cell cultures without CNTF (Fig. 2E). The presence of vesicular neurotransmitter transporters in the neuron-astrocyte generation suggests that another prerequisite for a functional network may have formed.

3.3. Neuron-astrocyte generation protocols alter neuron–astrocyte ratio

The ratio between neurons and astrocytes is an important factor influencing the functioning of a neuronal network. Fig. 3 presents the development of the neuron-astrocyte culture in terms of structural protein expression, gene expression relative to the NPC culture (at the stage just before differentiation) initiation, and spontaneous electrical activity in each of the four differentiation culture protocols.

P- cultures contained only a few GFAP$^+$ cells at day 14, which grew slightly in number over the course of the consecutive two weeks (Fig. 3A, P-). When enriched with CNTF, P + cultures presented a marked increase in cell number overall and in astrocytes in particular (Fig. 3A, P+). The G- protocol caused more cell growth in general and more astrocyte growth on day 28 as shown by more GFAP$^+$ cells compared to P- (Fig. 3A, G-). Supplementation with CNTF (G+) led to a sharp increase in cell numbers and in particular GFAP$^+$ astrocytes compared to P+ (Fig. 3A, G+).

Gene expression profiles largely followed the same pattern in all protocols: relative to NPCs, *POUF51* and *NEUROG1* expression

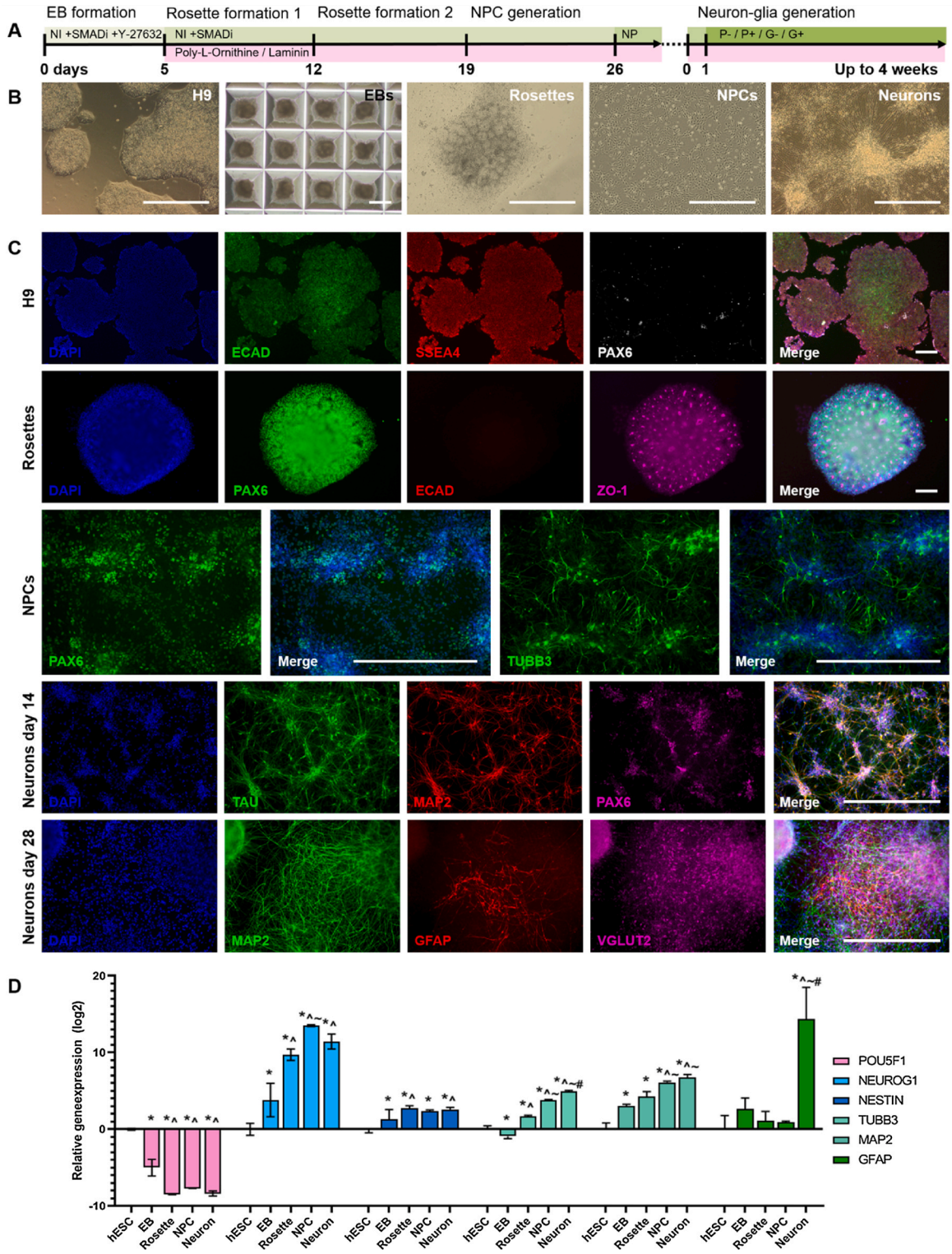

Fig. 1. Differentiation protocol of hESC into neural progenitors and subsequently into a network of neurons and astrocytes. (A) Protocol of NPC generation and neuron-astrocyte generation as described in Materials & Methods section. (B) Bright-field images showing the different stages of the differentiation process. (C) Characterisation of cell types present at different stages of differentiation with selected differentiation markers for stem cells (ECAD, SSEA-4), neural tube-like structures (ZO-1), NPCs (PAX6), immature neurons (TUBB3), axons (TAU), mature neurons/dendrites (MAP2), astrocytes (GFAP) and neurotransmitter vesicles (VGLUT2). (D) Relative gene expression changes throughout the NPC generation and differentiation shown by markers for stem cells (POU5F1), ectodermal differentiation (NEUROG1, NES), neurons (TUBB3, MAP2) and astrocytes (GFAP). Gene expression of all four differentiation protocols were combined in one bar ("Neuron"). Sample size: hESC n = 4, EB/NPC n = 2, Rosette n = 3, Neuron n = 23. NI: STEMdiff™ Neural Induction medium, NP: STEMdiff™ Neural Progenitor medium, P-/P+: neuron-astrocyte generation medium adopted from Pistollato et al. [23] without (-) and with (+) addition of CNTF, G-/+: medium from Gunhanlar et al. [24] without (-) and with(+) CNTF. Scale bar: 500 μm. Error bars: standard deviation. Significant difference ($p < 0.005$) from *: H9 stem cells, ^: EBs, ~: rosette, #: NPC.

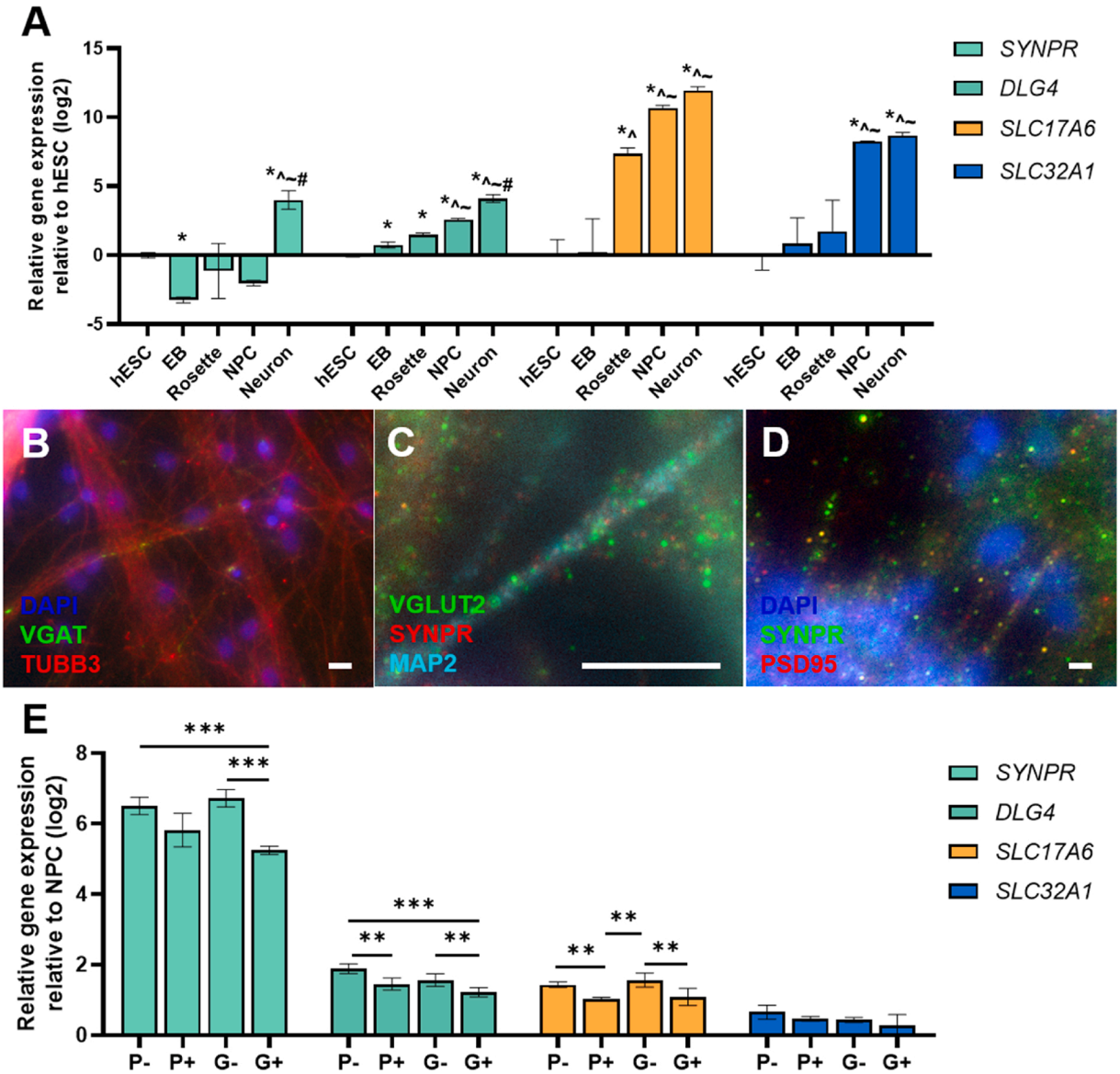

Fig. 2. Gene- and protein expression of transporters and synaptic proteins at various stages of differentiation. (A) Relative gene expression of synaptic- and transporter markers at each differentiation stage relative to the hESC culture. DLG4 gene encodes the PSD95 protein, SLC17A6 encodes VLGUT2, SLC32A1 encodes VGAT and SYNPR encodes SYNPR. (B)-(D) Immunostainings showing vesicle marker (B) VGAT at day 28, (C) vesicle marker VGLUT2 and synaptic marker SYNPR at day 14 and (D) synaptic markers PSD95 and SYNPR at day 28. (E) Day 14 gene expression of the four neuronal differentiation protocols relative to the NPC culture. P-, P+, G-, G + represent the four neuron-astrocyte generation protocols used. Sample size: hESC n = 4, EB/NPC n = 2, Rosette n = 3, Neuron n = 23 (P-/P + n = 5, G- n = 6, G + n = 7). Scale bar: 10 μm. Error bars: standard deviation. Significance: **: $p < 0.008$. ***: $<p < 0.0001$.

decreased, while *TUBB3, MAP2* and *GFAP* expression increased at day 14 (Fig. 3B). Of note is the lower upregulation of *TUBB3* in the G-protocols relative to P-, and the higher upregulation of *GFAP* with the addition of CNTF. This may suggest that astrocyte differentiation was increased at the expense of neural differentiation. Despite the strong upregulation of *GFAP*, protein expression seemed to be delayed in P- and G- (Fig. 3A). P + and G + cultures did show GFAP protein expression at day 14, although G + cultures contained more astrocytes, which could not be seen in the gene expression.

Spontaneous electrical activity developed under all culture conditions (Fig. 3C). Spontaneous activity for the majority of the protocols could be observed from day 3 after starting of differentiation on as single spikes across wells, and single spikes developed into spike trains and bursting activity within the first week. Activity generally increased steadily over time, although no synchronised network firing has been observed under the tested culture conditions.

The neuron-astrocyte cultures expressed relatively low spontaneous electrical activity. In order to improve the activity, half instead of full medium refreshments were performed at the same time interval as the full medium refreshments. Additionally, for P + and G+, CNTF was added only until day 8. Using this refreshment scheme, P- and G- cultures showed an increase in the number of $GFAP^{+}$ astrocytes at day 14 and 28, while in the P + and G + condition the opposite effect was observed (Suppl. Fig. 1). The MSR did not change with this refreshment regime, but the percentage of active wells increased to 90 % in the G + protocol, which was not observed in other culture conditions (Fig. 3D). The MBR and percentage of active wells showing bursting activity did not change.

The above results demonstrate that all culture conditions showed different ratios of neurons and astrocytes, and presented spontaneous electrical activity over time. These results were successfully repeated once within and once across cell banks.

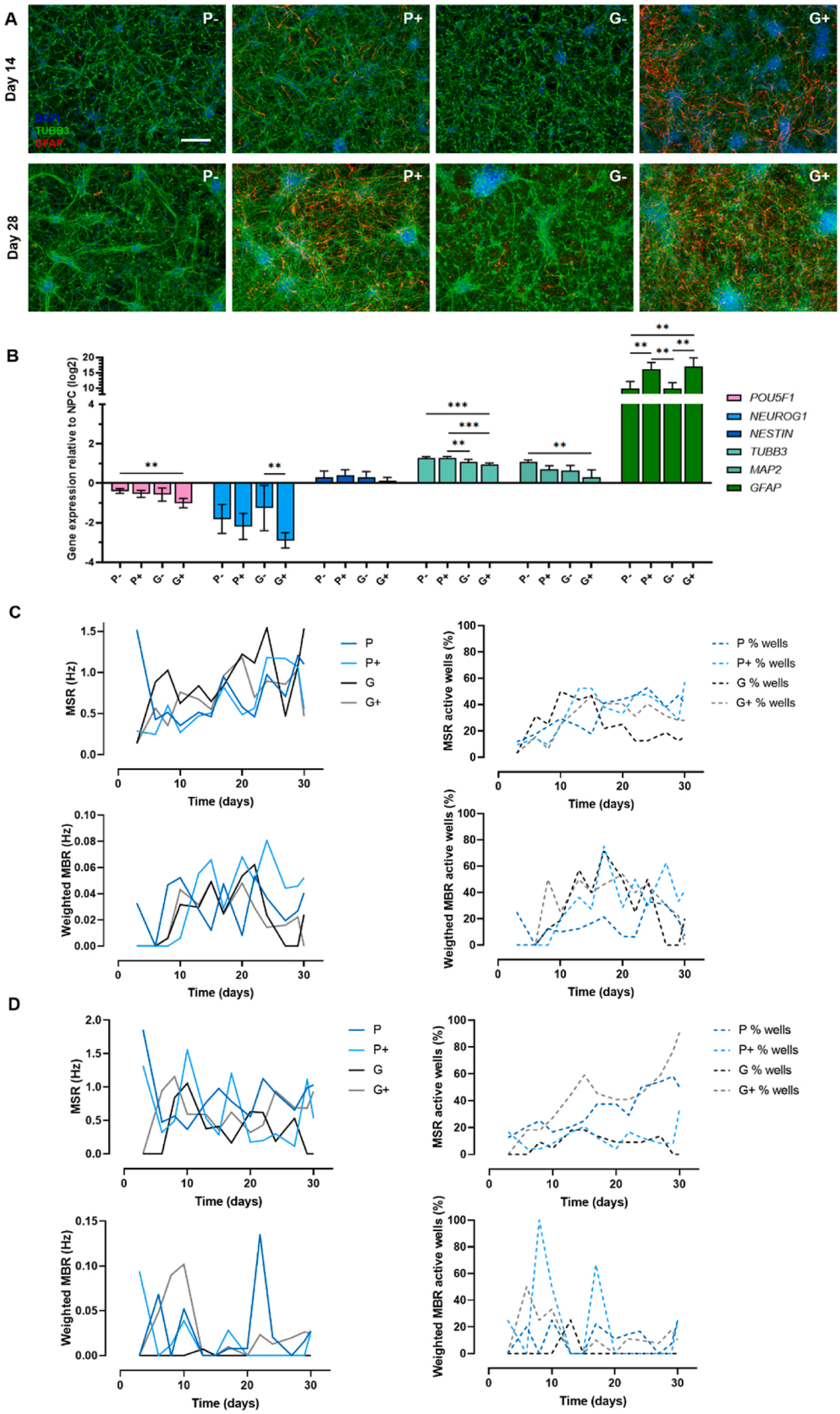

Fig. 3. Gene- and protein expression, and spontaneously firing of four differentiation protocols. (A) Immunostaining images of each of the protocols P-, P+, G-, G + on day 14 and day 28 of neurons (TUBB3, green) and astrocytes (GFAP, red). (B) Gene expression differences (log2) at day 14 relative to the NPC culture. (C) mwMEA measurements of mean spike rate (MSR) and weighted mean burst rate (MBR) in Hz per well of each of the protocols from day 3 until day 30 after full medium refreshments. Sample size P-/P+: N = 2, G-/G+: N = 3. (D) same as C, but after half medium refreshments and reduced CNTF exposure duration. Sample size P-/P+: N = 2, G-/G+: N = 3. Scale bar: 500 µm. Error bars: standard deviation. Significance: **: $p < 0.008$. ***: $p < 0.0001$ (For interpretation of the references to colour in this figure legend, the reader is referred to the web version of this article).

4. Discussion

In this study we presented an efficient protocol for the differentiation of NPCs into a spontaneously active network consisting of neurons and astrocytes. These NPCs were generated from hESCs in several consecutive steps (EBs; Rosettes and NPCs). Two NPC cell banks from two H9 aliquots have been generated and differentiation with these two different NPC banks based on protocols from other laboratories showed that the current protocol is robust and reproducible, which is important in the light of harmonisation of *in vitro* models for regulatory testing and implementation of DNT guidelines. Using qPCR and immunocytochemistry, the NPC generation and the neuron-astrocyte generation were characterized and showed a transition of hESCs and NPC through a number of phases that mimic key events in neuronal differentiation. In most protocols, within three days of neuron-astrocyte generation, cells were transformed into a mixture of excitatory neurons, inhibitory neurons and astrocytes that presented synaptic markers and showed spontaneous electrical activity over the course of multiple weeks, indicating a neural network, indicative of the development of a functional neuronal network. By testing four different protocols the neuron-astrocyte ratio could be modulated.

The observation of electrical activity in a differentiated neuronal culture indicates that a sufficient ratio of inhibitory and excitatory neurons is present and cells are functionally interacting in this model. This provides important added complexity as compared to the presence of cell differentiation markers per se. Many groups have shown the presence of prerequisites for a functional neuronal network, but failed to substantiate this with electrical activity as a functional readout [28–36]. Compared to other studies in which electrical activity was shown in hESC (H9 and other cell lines) and induced pluripotent stem cell (iPSC)-based differentiation protocols similar to our protocol, NPCs generated in this study developed spontaneous electrical activity considerably faster, typically within three days, versus one to five weeks in published studies [16,18,37–44]. In fact, only the study from Pistollato et al. [45] showed activity within one day in iPSC-derived neurons. Part of the current protocol was based on this Pistollato study, suggesting that this is a robust and reproducible protocol that works with different cell sources (H9 and iPSCs). The reason why activity occurred quickly in this study with hESC may be traced back to the second rosette selection in the differentiation of hESC into NPCs, which may have led to a select population of NPCs and early differentiating neurons that accelerated subsequent differentiation.

The levels of electrical activity shown in the present study were comparable to hESC-based models that were grown in a neurosphere configuration [16,37,46,43]. Cell models based on iPSCs [45,47] however showed 3–100 times higher maximum spontaneous firing and bursting activity. Rather than a direct readout for compound testing, the spontaneous electrical activity measured in this model provides an important basic proof of neuronal network quality as a prerequisite control condition for studying effects on biomarkers of neuronal differentiation and synaptogenesis.

The ratio between neurons and astrocytes is important for neuron maturation and firing function [47–49]. Furthermore, astrocytes are important for both endogenous and exogenous toxicity, e.g. by metabolising xenobiotics, which may affect their toxicity [50–52]. Our G + protocol with 50 % medium replacement and limited supplementation of CNTF resulted in the highest percentage of spiking wells among all protocols and therefore seems most promising for its intended purpose, i.e. a quickly differentiating neuron-astrocyte co-culture for compound-induced DNT assessment. By adding CNTF to the medium only during the first eight days of neuron-astrocyte generation, astrocytes could develop without overgrowing the neurons in the culture. By only changing half of the medium for every refreshment, the cells retained some of the local environment without being depleted of nutrients. This combination led to a steadily growing and maturing network without overgrowth of astrocytes. These observations support the important role of the neuron-astrocyte ratio in determining the extent of neuron firing in these cultures.

A single *in vitro* system will not suffice to replace the intact individual, especially in the case of the developing brain [53]. Therefore it is important to define the biological domain of an *in vitro* model, so that complementary assays can be joined in a testing strategy with broad coverage of mechanisms of action [2,3,54]. Based on the results on gene, protein and functional level, the differentiation from NPC to a neuron-astrocyte culture encompassed (early) differentiation of neurons and astrocytes, synaptogenesis and network formation [1]. Other major cell types in the brain such as oligodendrocytes and microglia are not likely to be present in this culture, which is a common challenge in these co-culture systems [3]. This may require a separate protocol starting from stem cells or NPCs and focusing on the generation of oligodendrocytes and / or microglia cells. To extend the detail of knowledge on the biological domain, research should focus on further characterisation of the model in terms of neuronal subtypes such as dopaminergic, cholinergic and serotonergic systems.

Characterisation of the neuron-astrocyte generation model with immunostainings and qPCR identified key processes in brain development such as neurite outgrowth, neuronal differentiation and glia formation. Within three days spontaneous electrical activity was observed that was maintained for several weeks, which confirmed formation of functional synapses, dendrite formation, balanced function of neuronal excitatory and inhibitory subtypes (glutamatergic and GABAergic) and neuronal maturation. This indicates that (most) prerequisites for development of a functional neuronal network were present. Future experiments will focus on the assessment of these essential endpoints to further delineate the biological domain of the model. This protocol may be used to efficiently predict DNT of compounds in a human relevant *in vitro* model mimicking essential processes in brain development.

Declaration of Competing Interest

The authors report no declarations of interest.

Acknowledgements

This research is funded by the Dutch NGO *Stichting Proefdiervrij* and the Dutch Ministry of Agriculture, Nature and Food Quality and the Dutch Ministry of Health, Welfare and Sports. We would like to thank Fiona Wijnolts, Anke Tukker and the rest of the Neurotoxicology team at IRAS (University Utrecht) for recording the MEA plates. We would like to thank Anne Kienhuis for a critical review of the manuscript.

Appendix A. Supplementary data

Supplementary material related to this article can be found, in the online version, at doi:https://doi.org/10.1016/j.reprotox.2020.09.003.

References

[1] E.V.S. Hessel, Y.C.M. Staal, A.H. Piersma, Design and validation of an ontology-driven animal-free testing strategy for developmental neurotoxicity testing, Toxicol. Appl. Pharmacol. 1 (2018) 136–152, https://doi.org/10.1016/j.taap.2018.03.013.

[2] E. Fritsche, P. Grandjean, K.M. Crofton, M. Aschner, A. Goldberg, T. Heinonen, E.V. S. Hessel, H.T. Hogberg, S.H. Bennekou, P.J. Lein, M. Leist, W.R. Mundy, M. Paparella, A.H. Piersma, M. Sachana, G. Schmuck, R. Solecki, A. Terron, F. Monnet-Tschudi, M.F. Wilks, H. Witters, M.G. Zurich, A. Bal-Price, Consensus statement on the need for innovation, transition and implementation of developmental neurotoxicity (DNT) testing for regulatory purposes, Toxicol. Appl. Pharmacol. 354 (2018) 3–6, https://doi.org/10.1016/j.taap.2018.02.004.

[3] A. Bal-Price, F. Pistollato, M. Sachana, S.K. Bopp, S. Munn, A. Worth, Strategies to improve the regulatory assessment of developmental neurotoxicity (DNT) using in vitro methods, Toxicol. Appl. Pharmacol. 354 (2018) 7–18, https://doi.org/10.1016/j.taap.2018.02.008.

[4] A. Thapar, M. Cooper, Attention deficit hyperactivity disorder, Lancet 387 (2016) 1240–1250, https://doi.org/10.1016/S0140-6736(15)00238-X.

[5] P. Grandjean, P.J. Landrigan, Neurobehavioural effects of developmental toxicity, Lancet Neurol. 13 (2014) 330–338, https://doi.org/10.1016/S1474-4422(13)70278-3.
[6] OECD, Test Guideline 426, OECD Guideline for Testing of Chemicals. Developmental Neurotoxicity Study, 2007. https://www.oecd-ilibrary.org/environment/test-no-426-developmental-neurotoxicity-study_9789264067394-en.
[7] OECD, Test Guideline 443, OECD Guideline for Testing of Chemicals, Extended One-generation Study, 2018. https://www.oecd-ilibrary.org/environment/test-no-443-extended-one-generation-reproductive-toxicity-study_9789264185371-en.
[8] A. Bal-Price, K.M. Crofton, M. Leist, S. Allen, M. Arand, T. Buetler, N. Delrue, R. E. FitzGerald, T. Hartung, T. Heinonen, H. Hogberg, S.H. Bennekou, W. Lichtensteiger, D. Oggier, M. Paparella, M. Axelstad, A. Piersma, E. Rached, B. Schilter, G. Schmuck, L. Stoppini, E. Tongiorgi, M. Tiramani, F. Monnet-Tschudi, M.F. Wilks, T. Ylikomi, E. Fritsche, International STakeholder NETwork (ISTNET): creating a developmental neurotoxicity (DNT) testing road map for regulatory purposes, Arch. Toxicol. 89 (2015) 269–287, https://doi.org/10.1007/s00204-015-1464-2.
[9] J.A. Harrill, B.L. Robinette, W.R. Mundy, Use of high content image analysis to detect chemical-induced changes in synaptogenesis in vitro, Toxicol. In Vitro 25 (2011) 368–387, https://doi.org/10.1016/j.tiv.2010.10.011.
[10] E. Taoufik, G. Kourouni, O. Zygogianni, R. Matsas, Synaptic dysfunction in neurodegenerative and neurodevelopmental diseases: an overview of induced pluripotent stem-cell-based disease models, Open Biol. 8 (2020) 180138, https://doi.org/10.1098/rsob.180138.
[11] N.E. Ziv, C.C. Garner, Cellular and molecular mechanisms of presynaptic assembly, Nat. Rev. Neurosci. 5 (2004) 385–399, https://doi.org/10.1038/nrn1370.
[12] C.L. Waites, A.M. Craig, C.C. Garner, Mechanisms of vertebrate synaptogenesis, Annu. Rev. Neurosci. 28 (2005) 251–274, https://doi.org/10.1146/annurev.neuro.27.070203.144336.
[13] E. Fritsche, M. Barenys, J. Klose, S. Masjosthusmann, L. Nimtz, M. Schmuck, S. Wuttke, J. Tigges, Development of the concept for stem cell-based developmental neurotoxicity evaluation, Toxicol. Sci. 165 (2018) 14–20, https://doi.org/10.1093/toxsci/kfy175.
[14] A.C. Feutz, C. De Geyter, Accuracy, discriminative properties and reliability of a human ESC-based in vitro toxicity assay to distinguish teratogens responsible for neural tube defects, Arch. Toxicol. 93 (2019) 2375–2384, https://doi.org/10.1007/s00204-019-02512-8.
[15] D. Pamies, A. Bal-Price, A. Simeonov, D. Tagle, D. Allen, D. Gerhold, D. Yin, F. Pistollato, T. Inutsuka, K. Sullivan, G. Stacey, H. Salem, M. Leist, M. Daneshian, M.C. Vemuri, R. Mcfarland, S. Coecke, S.C. Fitzpatrick, U. Lakshmipathy, A. Mack, W.B. Wang, D. Yamazaki, Y. Sekino, Y. Kanda, L. Smirnova, T. Hartung, Good cell culture practice for stem cells & stem-cell-derived models, ALTEX 34 (2017) 95–132, https://doi.org/10.14573/altex.1607121.
[16] M. Mayer, O. Arrizabalaga, F. Lieb, M. Ciba, S. Ritter, C. Thielemann, Electrophysiological investigation of human embryonic stem cell derived neurospheres using a novel spike detection algorithm, Biosens. Bioelectron. 100 (2018) 462–468, https://doi.org/10.1016/j.bios.2017.09.034.
[17] M. Barenys, K. Gassmann, C. Baksmeier, S. Heinz, I. Reverte, M. Schmuck, T. Temme, F. Bendt, T.C. Zschauer, T.D. Rockel, K. Unfried, W. Watjen, S. M. Sundaram, H. Heuer, M.T. Colomina, E. Fritsche, Epigallocatechin gallate (EGCG) inhibits adhesion and migration of neural progenitor cells in vitro, Arch. Toxicol. 91 (2016) 827–837, https://doi.org/10.1007/s00204-016-1709-8.
[18] T. Paavilainen, A. Pelkonen, M.E.-L. Mäkinen, M. Peltola, H. Huhtala, D. Fayuk, S. Narkilahti, Effect of prolonged differentiation on functional maturation of human pluripotent stem cell-derived neuronal cultures, Stem Cell Res. 27 (2018) 151–161, https://doi.org/10.1016/J.SCR.2018.01.018.
[19] B.Z. Schmidt, M. Lehmann, S. Gutbier, E. Nembo, S. Noel, L. Smirnova, A. Forsby, J. Hescheler, H.X. Avci, T. Hartung, M. Leist, J. Kobolák, A. Dinnyés, In vitro acute and developmental neurotoxicity screening: an overview of cellular platforms and high-throughput technical possibilities, Arch. Toxicol. 91 (2017) 1–33, https://doi.org/10.1007/s00204-016-1805-9.
[20] M. Telias, D. Ben-Yosef, Modeling neurodevelopmental disorders using human pluripotent stem cells, Stem Cell Rev. Reports 10 (2014) 494–511, https://doi.org/10.1007/s12015-014-9507-2.
[21] D.M. Panchision, The role of oxygen in regulating neural stem cells in development and disease, J. Cell. Physiol. 220 (2009) 562–568, https://doi.org/10.1002/jcp.21812.
[22] D. Lukmanto, V.C. Khanh, S. Shirota, T. Kato, M.M. Takasaki, O. Ohneda, Dynamic changes of mouse embryonic stem cell-derived neural stem cells under in vitro prolonged culture and hypoxic conditions, Stem Cells Dev. 28 (2019) 1434–1450, https://doi.org/10.1089/scd.2019.0101.
[23] F. Pistollato, D. Canovas-Jorda, D. Zagoura, A. Price, Protocol for the differentiation of human induced pluripotent stem cells into mixed cultures of neurons and glia for neurotoxicity testing, J. Vis. Exp. 2017 (2017) e55702, https://doi.org/10.3791/55702.
[24] N. Gunhanlar, G. Shpak, M. van der Kroeg, L.A. Gouty-Colomer, S.T. Munshi, B. Lendemeijer, M. Ghazvini, C. Dupont, W.J.G. Hoogendijk, J. Gribnau, F.M.S. de Vrij, S.A. Kushner, A simplified protocol for differentiation of electrophysiologically mature neuronal networks from human induced pluripotent stem cells, Mol. Psychiatry 23 (2018) 1336–1344, https://doi.org/10.1038/mp.2017.56.
[25] W.S. Rasband, ImageJ, U. S. Natl. Institutes Heal. Bethesda, Maryland, USA. (n.d.). https://imagej.nih.gov/ij/.
[26] Applied Biosystems, User Bulletin #2 ABI PRISM 7700 Sequence Detection System, 2001, pp. 1–36. http://tools.thermofisher.com/content/sfs/manuals/cms_040980.pdf.
[27] A.M. Tukker, M.W.G.D.M. De Groot, F.M.J. Wijnolts, E.J. Emma, L. Hondebrink, R. H.S. Westerink, Is the time right for in vitro neurotoxicity testing using human iPSC-derived neurons? ALTEX 33 (2016) 261–271, https://doi.org/10.14573/altex.1510091.
[28] S.C. Zhang, M. Wernig, I.D. Duncan, O. Brustle, J.A. Thomson, In vitro differentiation of transplantable neural precursors from human embryonic stem cells, Nat. Biotechnol. 19 (2001) 1129–1133, https://doi.org/10.1038/nbt1201-1129.
[29] B.E. Reubinoff, M.F. Pera, C.Y. Fong, A. Trounson, A. Bongso, Embryonic stem cell lines from human blastocysts: somatic differentiation in vitro, Nat. Biotechnol. 18 (2000) 399–404, https://doi.org/10.1038/74447.
[30] S. Colleoni, C. Galli, S.G. Giannelli, M.T. Armentero, F. Blandini, V. Broccoli, G. Lazzari, Long-term culture and differentiation of CNS precursors derived from anterior human neural rosettes following exposure to ventralizing factors, Exp. Cell Res. 316 (2010) 1148–1158, https://doi.org/10.1016/j.yexcr.2010.02.013.
[31] O. Sterthaus, A.C. Feutz, H. Zhang, F. Pletscher, E. Bruder, P. Miny, G. Lezzi, M. De Geyter, C. De Geyter, Gene expression profiles of similarly derived human embryonic stem cell lines correlate with their distinct propensity to exit stemness and their different differentiation behavior in culture, Cell. Reprogram. 16 (2014) 185–195, https://doi.org/10.1089/cell.2013.0089.
[32] L. Buzanska, J. Sypecka, S. Nerini-Molteni, A. Compagnoni, H.T. Hogberg, R. Del Torchio, K. Domanska-Janik, J. Zimmer, S. Coecke, A human stem cell-based model for identifying adverse effects of organic and inorganic chemicals on the developing nervous system, Stem Cells 27 (2009) 2591–2601, https://doi.org/10.1002/stem.179.
[33] R. Taléns-Visconti, I. Sanchez-Vera, J. Kostic, M.A. Perez-Arago, S. Erceg, M. Stojkovic, C. Guerri, Neural differentiation from human embryonic stem cells as a tool to study early brain development and the neuroteratogenic effects of ethanol, Stem Cells Dev. 20 (2011) 327–339, https://doi.org/10.1089/scd.2010.0037.
[34] M.P. Schwartz, Z. Hou, N.E. Propson, J. Zhang, C.J. Engstrom, V.S. Costa, P. Jiang, B.K. Nguyen, J.M. Bolin, W. Daly, Y. Wang, R. Stewart, C.D. Page, W.L. Murphy, J. A. Thomson, Human pluripotent stem cell-derived neural constructs for predicting neural toxicity, Proc. Natl. Acad. Sci. U. S. A. 112 (2015) 12516–12521, https://doi.org/10.1073/pnas.1516645112.
[35] A.K. Krug, R. Kolde, J.A. Gaspar, E. Rempel, N.V. Balmer, K. Meganathan, K. Vojnits, M. Baquié, T. Waldmann, R. Ensenat-Waser, S. Jagtap, R.M. Evans, S. Julien, H. Peterson, D. Zagoura, S. Kadereit, D. Gerhard, I. Sotiriadou, M. Heke, K. Natarajan, M. Henry, J. Winkler, R. Marchan, L. Stoppini, S. Bosgra, J. Westerhout, M. Verwei, J. Vilo, A. Kortenkamp, J. Hescheler, L. Hothorn, S. Bremer, C. Van Thriel, K.H. Krause, J.G. Hengstler, J. Rahnenführer, M. Leist, A. Sachinidis, Human embryonic stem cell-derived test systems for developmental neurotoxicity: a transcriptomics approach, Arch. Toxicol. 87 (2013) 123–143, https://doi.org/10.1007/s00204-012-0967-3.
[36] C.R. Muratore, P. Srikanth, D.G. Callahan, T.L. Young-Pearse, Comparison and optimization of hiPSC forebrain cortical differentiation protocols, PLoS One 9 (2014) e105807, https://doi.org/10.1371/journal.pone.0105807.
[37] A. Hyysalo, M. Ristola, M.E.-L. Mäkinen, S. Häyrynen, M. Nykter, S. Narkilahti, Laminin α5 substrates promote survival, network formation and functional development of human pluripotent stem cell-derived neurons in vitro, Stem Cell Res. 24 (2017) 118–127, https://doi.org/10.1016/j.scr.2017.09.002.
[38] J.-E. Kim, M.L. Sullivan, C.A. Sanchez, M. Hwang, M.A. Israel, K. Brennand, T. J. Deerinck, L.S.B. Goldstein, F.H. Gage, M.H. Ellisman, A. Ghosh, Investigating synapse formation and function using human pluripotent stem cell-derived neurons, Proc. Natl. Acad. Sci. 108 (2011) 3005–3010, https://doi.org/10.1073/pnas.1007753108.
[39] M.K. Carpenter, M.S. Inokuma, J. Denham, T. Mujtaba, C.P. Chiu, M.S. Rao, Enrichment of neurons and neural precursors from human embryonic stem cells, Exp. Neurol. 172 (2001) 383–397, https://doi.org/10.1006/exnr.2001.7832.
[40] S.K. Goparaju, K. Kohda, K. Ibata, A. Soma, Y. Nakatake, T. Akiyama, S. Wakabayashi, M. Matsushita, M. Sakota, H. Kimura, M. Yuzaki, S.B.H. Ko, M.S. H. Ko, Rapid differentiation of human pluripotent stem cells into functional neurons by mRNAs encoding transcription factors, Sci. Rep. 7 (2017) 42367, https://doi.org/10.1038/srep42367.
[41] A. Chandrasekaran, H.X. Avci, A. Ochalek, L.N. Rösingh, K. Molnár, L. László, T. Bellák, A. Téglási, K. Pesti, A. Mike, P. Phanthong, O. Bíró, V. Hall, N. Kitiyanant, K.H. Krause, J. Kobolák, A. Dinnyés, Comparison of 2D and 3D neural induction methods for the generation of neural progenitor cells from human induced pluripotent stem cells, Stem Cell Res. 25 (2017) 139–151, https://doi.org/10.1016/j.scr.2017.10.010.
[42] R. Lieberman, E.S. Levine, H.R. Kranzler, C. Abreu, J. Covault, Pilot study of iPS-derived neural cells to examine biologic effects of alcohol on human neurons in vitro, Alcohol. Clin. Exp. Res. 36 (2012) 1678–1687, https://doi.org/10.1111/j.1530-0277.2012.01792.x.
[43] J. Sandström, E. Eggermann, I. Charvet, A. Roux, N. Toni, C. Greggio, A. Broyer, F. Monnet-Tschudi, L. Stoppini, Development and characterization of a human embryonic stem cell-derived 3D neural tissue model for neurotoxicity testing, Toxicol. In Vitro 38 (2017) 124–135, https://doi.org/10.1016/j.tiv.2016.10.001.
[44] L. D'Aiuto, Y. Zhi, D. Kumar Das, M.R. Wilcox, J.W. Johnson, L. McClain, M. L. MacDonald, R. Di Maio, M.E. Schurdak, P. Piazza, L. Viggiano, R. Sweet, P. R. Kinchington, A.G. Bhattacharjee, R. Yolken, V.L. Nimgaonkar, Large-scale generation of human iPSC-derived neural stem cells/early neural progenitor cells and their neuronal differentiation, Organogenesis 10 (2014) 365–377, https://doi.org/10.1080/15476278.2015.1011921.
[45] F. Pistollato, D. Canovas-Jorda, D. Zagoura, A. Bal-Price, Nrf2 pathway activation upon rotenone treatment in human iPSC- derived neural stem cells undergoing

differentiation towards neurons and astrocytes, Neurochem. Int. 108 (2017) 457–471, https://doi.org/10.1016/j.neuint.2017.06.006.
[46] T.J. Heikkilä, L. Ylä-Outinen, J.M.A. Tanskanen, R.S. Lappalainen, H. Skottman, R. Suuronen, J.E. Mikkonen, J.A.K. Hyttinen, S. Narkilahti, Human embryonic stem cell-derived neuronal cells form spontaneously active neuronal networks in vitro, Exp. Neurol. 218 (2009) 109–116, https://doi.org/10.1016/j.expneurol.2009.04.011.
[47] A.M. Tukker, F.M.J. Wijnolts, A. de Groot, R.H.S. Westerink, Human iPSC-derived neuronal models for in vitro neurotoxicity assessment, Neurotoxicology 67 (2018) 215–225, https://doi.org/10.1016/j.neuro.2018.06.007.
[48] L.E. Clarke, B.A. Barres, Emerging roles of astrocytes in neural circuit development, Nat. Rev. Neurosci. 14 (2013) 311–321, https://doi.org/10.1038/nrn3484.
[49] M. Amiri, N. Hosseinmardi, F. Bahrami, M. Janahmadi, Astrocyte- neuron interaction as a mechanism responsible for generation of neural synchrony: a study based on modeling and experiments, J. Comput. Neurosci. 34 (2013) 489–504, https://doi.org/10.1007/s10827-012-0432-6.
[50] T. Ishii, E. Kawakami, K. Endo, H. Misawa, K. Watabe, Myelinating cocultures of rodent stem cell line-derived neurons and immortalized Schwann cells, Neuropathology 37 (2017) 475–481, https://doi.org/10.1111/neup.12397.
[51] T. Takemoto, Y. Ishihara, A. Ishida, T. Yamazaki, Neuroprotection elicited by nerve growth factor and brain-derived neurotrophic factor released from astrocytes in response to methylmercury, Environ. Toxicol. Pharmacol. 40 (2015) 199–205, https://doi.org/10.1016/J.ETAP.2015.06.010.
[52] P. Bajpai, M.C. Sangar, S. Singh, W. Tang, S. Bansal, G. Chowdhury, Q. Cheng, J. K. Fang, M.V. Martin, F.P. Guengerich, N.G. Avadhani, Metabolism of 1-methyl-4-phenyl-1,2,3/6-tetrahydropyridine by mitochondrion-targeted cytochrome P450 2D6 implications in parkinson disease, J. Biol. Chem. 288 (2013) 4436–4451, https://doi.org/10.1074/jbc.M112.402123.
[53] T. Hartung, H. Hodgberg, M. Leist, D. Pamies, L. Smirnova, Advanced cell techniques to study developmental neurobiology and toxicology. Neural Cell Biol., CRC Press, Boca Raton, FL, USA, 2017, pp. 187–217, https://doi.org/10.1201/9781315370491.
[54] M. Sachana, A. Bal-Price, K.M. Crofton, S.H. Bennekou, T.J. Shafer, M. Behl, A. Terron, International regulatory and scientific effort for improved developmental neurotoxicity testing, Toxicol. Sci. 167 (2019) 45–57, https://doi.org/10.1093/toxsci/kfy211.